ISSN : 0974 - 7435 Volume 10 Issue 20

2014

BioTechnology
An Indian Journal

FULL PAPER

BTAIJ, 10(20), 2014 [12311-12317]

# Application of image processing in assembly detection of large complex precision components based on machine vision technology

Xiaoyun Zhang[1], Yubin Liu[2], Yucheng Liu[1*]
[1]College of Electrical & Information Engineering, Chongqing University of Science & Technology, Chongqing, Shapingba, 401331, (CHINA)
[2]School of Continuing Education, Panzhihua Univerisity, Sichuan, Panzhihua, 617000, (CHINA)
E-mail: Lych68782763@163.com

## ABSTRACT

Aimed at human vision not being able to meet the requirement of the non-defect work-piece inspection in the large complex precision components assembly, the paper put forward an image processing method to realize the scathe-less detection of the work-piece by the industrial computerized tomography (CT) image. This method uses the industrial CT image to make the scathe-less detection for each work-piece and applies phase correlation method to realize location of the same section position CT image using Hausdorff distance. Finally, using the position information which template image located in the original image, to judge the assembly is right or not. In this paper, it took the recognition inspection of precision assembly of metal parts as an example that judged the location information in the original image by means of template image. The judged results showed that the correct recognition rate of the part assembly was 100%.

## KEYWORDS

Industrial computerized tomography image; Non-defect work-piece; Image processing; Hausdorff distance; Phase correlation method.

## INTRODUCTION

The characteristics of the machine vision system are to improve the flexibility and automation degree of the production. In some dangerous work environment for the human vision to be difficult to meet the requirement, machine vision is often used to replace the human vision. In the mass industrial production process, the human vision inspection of the product quality is low in the efficiency and is not high in the accuracy, while the machine vision detection method can greatly improve the efficiency and automation degree of the production. And the machine vision is easy to realize information integration. This paper roughly explored the related technical problems of machine vision application in the assemble inspection of complex metal parts from the point of view of applications.

## SCATHE-LESS INSPECTION OF INDUSTRIAL CT IMAGE

The machine vision system is a kind of product integrated device of software and hardware, which can transform the taken target into the image signal, and then transfer it to a special information device to make further processing. At the present, the industrial CT image detect is mainly completed by handwork method. It is difficult to satisfy a lot of image processing needs. The paper discusses an auto-detect method based on image edge.

## INSPECTION PRINCIPLE

The work-piece defect is relative. According to different purpose, it is not the same in extent and range and position of allowable defect, and some work-piece do not allow any defect at all. Therefore how to identify the defects is the key to decide the component whether practicable. The general method is that it gets the fault image of metal work-piece by industrial CT machine firstly, then considering from the angle of signal sample, the passing photon of inspected work-piece is transformed into analog signal through sensor, and after that it is transformed into the digital signal by means of A/D conversion. In the above process, the area edge which is from different material of original work-piece is different. On the basis of reconstruction algorithm of reverse projection in CT convolution, we can know that the pixels of edge range of real boundary are greater than or equal to 3 pixels in the digital image. A good edge detect operator should own such indices as low in misplay probability, high in location precision and uniqueness in each edge response. For this reason, Canny presented three criteria judged the edge inspection operator[1].

(i)Signal-noise ratio. The criterion is that it is lower in probability judged non-edge point as the edge point and judged edge point as non-edge point. The math expression of signal-noise ratio is Eq.1.

$$SNR = \left| \int_{-\omega}^{+\omega} G(-x) f(x) dx \right| / \left(\sigma \sqrt{\int_{-\omega}^{+\omega} f^2(x) dx}\right) \tag{1}$$

In which, $f(x)$ is pulse response of filter bounded over $[-\omega,+\omega]$, G(-x) represents the edge function, σ is the unbiased variance of Gaussian noise, if signal-noise ratio is big then it is better in edge extract quality.

(ii) Criterion of located precision. The location precision shows that the inspected edge point should be located the center of practical edge as far as possible. It can be expressed as Eq.2.

$$Localization = \left| \int_{-\omega}^{+\omega} G'(x) f'(x) dx \right| / \left(\sigma \sqrt{\int_{-\omega}^{+\omega} f'^2(x) dx}\right) \tag{2}$$

In which, $G'(x)$ and $f'(x)$ respectively represents first–order derivate of $G(x)$ and $f(x)$. If the value of Localization is bigger, then it shows the location precision will be high.

(iii) Criterion of single-side response. Namely if it wants to ensure that there is only one image in single-side edge, then the average distance of inspection operator of zero cross point of pulse response derivative should satisfy Eq.3.

$$D(f') = \pi \sqrt{\int_{-\infty}^{+\infty} f'^2(x) dx / \int_{-w}^{+w} f''(x) dx} \tag{3}$$

In which, $f''(x)$ is second-order derivative of $f(x)$.

## CANNY ALGORITHM OF EDGE INSPECTION

In the Canny algorithm, the method of two-door to limit is used to realize edge extracting, in which the two-door to limit is respectively the h1 and h2. And Canny suggests h2 should be 2～3 times of h1. The algorithm steps is as the following.

Step1: To initialize the location of edge dot, Edge Dot = (col, vol), col=0, vol=0. and define the figure edge array is nWidth×nHeight, all are initialized to be as 255 (for non-edge).

Step2: To examine the value of Edge Dot in the got figure of non-maximum suppression and give the value of IfEdge.

Step3: If (IfEdge=noedge) then Step7.

Step4: To examine value of EdgeDot in the gradient figure and give the value of magnitude.

Step5: If (magnitude<h2) then Step7.

Step6: Record EdgeDot in the edge figure, and set the value of corresponding dot, which is located in figure of non-maximum suppression to be as noedge. Then examine gradient value of magnitudenear of eight other domains of EdgeDot in the gradient figure, if magnitudenear is great than h1 then repeat to execute Step6, else execute Step7.

Step7: col++;

If (col>=nWidth) then vol++;

If (vol>=nHeight) then end;

Execute Step2.

In the above algorithm, the selection of threshold will directly influence the performance of Canny operator.

By Visual C++ 6.0, the above algorithm was realized. The algorithm consists of the following steps such as image smoothing (Gaussian filtering), differentiation processing, non-maximum suppression, edge threshold, etc. It selected a section in the CT image series, the effect of engineering application is shown as in Figure 1 by image segmentation method.

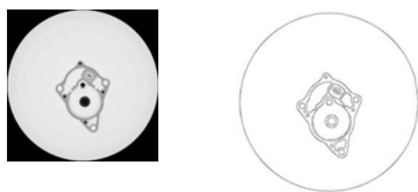

(a) CT original image (b) CT edge image

**Figure 1 : Extract effect of industrial edge for multi-materials**

## AUTO-DETECTION OF IMAGE

In the image of industrial CT, the substance of different area always is represented as gray level that is different from around substance. Therefore it can be separated from that area by the techniques of edge inspection and image segmentation, and it can be viewed as an independent analysis object. After that, it can be measured accurately. At present, the area detect is mainly completed by handwork manner. This kind of detect method always brings about more error because of artificial reason and itself defect of the algorithm, and it does not possess repeatable manipulation, and therefore it is difficult to realize image detect group by group[2]. But the image can be well and truly segmented to get its edge, and by means of auto-detect of CT image, the size can be realized such as area, circumference and extremum diameter, etc.

(i) Area detection. Because the regional area is only related to the regional boundary of the image, it can be computed by means of coordinate. The Green theorem pointed out that the surround area of a closed curve is determined by its outline integral in the x-y plane as shown in Eq.4.

$$A = \oint (xdy - ydx)/2 \quad \textbf{(4)}$$

In which the integral carries through along the closed curve. The discrete Green theorem is shown as in Eq.5.

$$\mathrm{A} = \sum_{i=1}^{N_b} [x_i y_{i+1} - x_{i+1} y_i]/2 \quad \textbf{(5)}$$

(ii) Circumference detection. It is the boundary length of segmented region. Here only chain code detect method is used. There are eight possible directions. Therefore the identifier can be specified from 0 to 7 as shown in Figure 2. It consists of start coordinate and code sequence that determine the pass trend around the boundary. In this boundary chain code, the pixel 0,2,4 and 6 is called as even step pixel, and the pixel 1,3,5 and 7 is called as odd step pixel.

| | | |
|---|---|---|
| 3 | 2 | 1 |
| 4 | | 0 |
| 5 | 6 | 7 |

**Figure 2 : Boundary Chain code**

The method of computing circumference is that firstly the region boundary is defined as a polygon which is the vertex centered by pixel center of each boundary, then the responding circumference is the sum of the space of a series of horizontal & vertical direction ($\Delta p_1 = 1$) and diagonal direction ($\Delta p_2 = \sqrt{2}$). A circumference with defect can be represented as Eq.6.

$$p = N_e + \sqrt{2} N_0 \tag{6}$$

In which, $N_e$ and $N_o$ is respectively to show the number of even step (0, 2, 4, 6) and odd step (1, 3, 5, 7) specified in the boundary chain code.

(iii) Extremum diameter. The extremum diameter of each point in the region is defined as the distance from geometrical center of the region to boundary point of region. It can get the discrete form of geometry center in arbitrary region by use of Green theorem and geometry center algorithm of the triangle, shown as in Eq.7 and Eq. 8.

$$x_i = \sum_{i=0}^{N_b} (x_{i+1} + x_i)(x_i y_{i+1} + x_{i+1} y_i)/3 \tag{7}$$

$$y_i = \sum_{i=0}^{N_b} (y_{i+1} + y_i)(x_i y_{i+1} + x_{i+1} y_i)/3 \tag{8}$$

(iv)Auto-detect of parameters. The steps are is the following: to gain the edge image of industrial CT automatically; to search all the closed and non-closed curves of edge image automatically; to create the region of all different quality materials in the industrial CT image and to mark the trajectory of all non-closed curve by use of all the closed curve; to identify the different region and to detect the area, circumference and extremum diameter. Based on the above scathe-less inspection of industrial CT, it is verified that it can reach to 97.6% in area average precision, and 98.2% in circumference, and 100% in extremum diameter in standard circle and ellipse image. For auto-detect time of all the size CT image, the large the image area is, the longer the creating image time is, and accordingly the longer the detect time is. For example, a 1500 breadths of batch CT image for a certain given work-piece, all the detect time only take 17 minutes.

## ASSEMBLY INSPECTION BASED ON MACHINE VISION

### Image registration

There are lots of image registration methods. Here it is only discussed to the Fourier based translation method so as to carry through the registration.

(1) Translation. If $f_2$(x, y) is the image of $f_1$(x, y) after translated ($x_0$, $y_0$), namely $f_2(x, y) = f_1(x\text{-}x_0, y\text{-}y_0)$ then the Fourier-based translation relationship between $F_1$ and $F_2$ is correspondingly shown as in Eq.9.

$$F_2(\xi, \eta) = e^{-j2\pi(\xi x_0 + \eta y_0)} F_1(\xi, \eta) \tag{9}$$

And the mutual energy spectrum of two images in corresponding frequency domain is as shown in Eq.10.

$$\frac{F_1(\xi,\eta)F_2^*}{\left|F_1(\xi,\eta)F_2^*\right|} = e^{j2\pi(\xi x_0 + \eta y_0)} \tag{10}$$

In which, $F_2^*$ is complex conjugation of $F_2$. By means of inverse transformation of mutual energy spectrum, it can get a pulse function $\delta(x - x_0, y - y_0)$. And it has an obvious sharp peak value in the shifting position, and it is near to zero in the other position. Therefore based on that, the deviation between images can be found.

(2) Rotation characteristic. If $f_2(x, y)$ is the image of $f_1(x, y)$ after translated $(x_0, y_0)$ and rotating $\theta_0$, namely $f_2(x,y) = f_1(x\cos\theta_0 + y\sin\theta_0 - x_0, -x\sin\theta_0 + y\cos\theta_0 - y_0)$, the relation between two images after transformation is as shown in Eq.11

$$F_2(\xi,\eta) = e^{-j2\pi(\xi x_0 + \eta y_0)} F_1(\xi\cos\theta_0 + \eta\sin\theta_0, -\xi\sin\theta_0 + \eta\cos\theta_0) \qquad \textbf{(11)}$$

Assume $M_1$ and $M_2$ is respectively the energy of $F_1$ and $F_2$, then Eq.12 holds.

$$M_2(\xi,\eta) = M_1(\xi\cos\theta_0 + \eta\sin\theta_0, -\xi\sin\theta_0 + \eta\cos\theta_0) \qquad \textbf{(12)}$$

Eq.12 in polar coordinate can be described as Eq.13.

$$M_1(\rho,\theta) = M_2(\rho,\theta - \theta_0) \qquad \textbf{(13)}$$

By use of the phase correlation theory, $\theta_0$ can be obtained.

In order to verify the effect of the selected algorithm, here it took three pieces of CT images to make image registration experience. Figure 3(a) is the original image, and it will be considered as reference image. Figure 3(b) is the image, in which there is not any rotation and translation. Figure 3(c) is the image, in which there is only rotation. The practical image registration results show that it is higher in precision, and smaller in gray scale influence, and insensitive in random noise[3].



(a) Original CT image (b) image in being rotation (c) image in being rotation and translation

**Figure 3 : Image registration**

**location of image registration**

The template match is a sort of important method in the image location. The paper takes Hausdorff distance of low and middle level characteristic to be as the similarity measure.

(1) Hausdorff distance. Hausdorff distance is a sort of max-min distance defined over two-dot set. Given a definite two-dot set, A = $\{a_1,\ldots,a_p\}$ and B=$\{b_1,\ldots, bq\}$, then Hausdorff distance between A and B is defined as Eq.14.

$$H(\mathrm{A},\mathrm{B})=\max(h(\mathrm{A},\mathrm{B}),h(\mathrm{B},\mathrm{A})) \qquad \textbf{(14)}$$

In which, $h$ (A, B) is called unidirectional Hausdorff distance. $h(A,B) = \max_{a\in A}\min_{b\in B} \| a-b \|$, where $\|\cdot\|$ is the normal form of distance between dot set A and dot set B (such as Euclidean distance. The Eq.14 is called as bidirectional Hausdorff distance, and it is a basic form of Hausdorff distance. The Hausdorff distance is always used for the template matching of binary image. The image edge characteristic is generally taken as the matching base. After the edge of detected image and template is respectively extracted, the matching location is determined by Hausdorff distance between two binary images. Assume that the pixel dot set of detected edge image is I =$\{i_1, i_2, \ldots,i_p\}$, and the characteristic dot set of template is M = $\{m_1,m_2,\ldots m_q\}$, then the bidirectional Hausdorff distance between template and image is $H$(M,I)= max($h$(M,I),$h$(I,M)). In which, $h$(M, I) is the distance from template to image, and $h$(I,M) is the distance from image to template. In this paper, the improved computing formula of unidirectional Hausdorff distance was proposed as shown in Eq.15.

$$h(A,B) = \sum_{a\in A}\min_{b\in B} \| a-b \| / N_A \qquad \textbf{(15)}$$

In which, $N_A$ is the number in the dot set of A.

(2)Edge extract. In the paper, the image edge is extracted by Canny edge inspection operator. Its advantages are that it can not only find the edge location information, but also it can get the direction information of edge image pixel, and each edge responses only once. By means of Canny edge inspection operator, it is more complete in extracting edge, the extracted edge can be used to process the following-up matching location.

(3)Hausdorff distance of target matching. In the paper, Chamfer distance transformation is used, in which the template image carries through translation matching over distance map. Accordingly, $h_j(M, I)$ can take the maximum in a certain number of corresponding location which is edge pixel dot of template image in the current distance map, it is the most dis-matching detect of template image between current translation location and corresponding pixel dot of edge image. And then the judge rule of Hausdorff distance template matching in basic form is that it takes the minimum in the above $h_j(M,I)$value got from all the translation matching to be as the similarity measure between the template and template corresponding target which exists probably in the image[4-5]. In the paper, a matching method of modified Hausdorff distance is that firstly it can find the average value got from each translation then it can obtain the similarity of corresponding waited recognition image in the template. The value of similarity minimum location is the most possible appeared location in template image. To compare its location coordinate ($x$, $y$) with the coordinate in the reference image of template image, if all the differences of horizontal and vertical coordinate are less than presetting threshold value then it is considered as that there is template image in the waited inspection image, and the assembly is correct, and otherwise it is considered as assembly fault.

**Experiment result**

The above algorithm is realized by VISUAL C++6.0. Figure 4 is the part image to be located. Figure 5 is the edge image after image registration. Figure 6 is the result image after matching location of image registration. To verify algorithm effectiveness by use of Hausdorff distance carried through matching location, Figure 3(b) and Figure 3(c) was modified, the located component was removed. The recognition result was shown in TABLE 1.

**Figure 4 : Template image**

**Figure 5 : Edge image after registration**

**Figure 6 : Image after location**

**TABLE 1 : Recognition inspection result**

| | Template location | Measured | Location | Template | Inspection |
|---|---|---|---|---|---|
| Figure 3(b) | (240,240) | (241,241) | (3,3) | yes | correct |
| Figure 3(c) | | (242,240) | | yes | correct |
| Gray draw in Figure 3(b) | | (241,241) | | yes | correct |
| Add random noise in Figure 3(c) | | (242,240) | | yes | correct |
| Remove template in Figure 3(b) | Non-existent | (286,253) | | no | correct |
| Remove template in Figure 3(c) | | (226,293) | | no | correct |

## DISCUSSION

It is known from TABLE 1 that it can carry through correct recognition whether the component assembly is correct or leak assembly by means of presented recognition inspection algorithm. The experiment result shows that the defect recognition of component assembly is feasible and effective, and it is stronger in anti-jamming and fault-tolerant performance, therefore it provides a sort of salutary mirror.

## ACKNOWLEDGEMENT

This study was supported by natural science foundation of Chongqing Yongchuan (Grant No. YCSTC, 2013nc8003), research Foundation of Chongqing municipal education committee (Grant No.KJ1401333), national natural science foundation of China (Grant No. 51105398).

## REFERENCES

[1] J.Canny; A computational approach to edge detection, IEEE Transactions on Pattern Analysis and Machine Intelligence, **8(6)**, 679-698 **(1986)**.

[2] J.D.Yang, J.H.Yang; improved approach to global localization based on odometry error modeling for mobile robots, Applied Mathematics & Information Sciences **8**, 563–576 **(2014)**.

[3] A.D.Deng, H.Tong, J.N.Tang, H.Cao; study on location algorithms of beamforming based on MVDR, Applied Mathematics & Information Sciences, **7**, 2455–2466 **(2013)**.

[4] J.R.Fram, E.S.Deutsch; On the quantitative evaluation of edge detection schemes and their comparison with human performance, IEEE Trans.Comput.C., **24(6)**, 616–628 **(1995)**.

[5] H.S.Stone, R.Wolpov; Blind cross-spectral image registration using prefiltering and fourier-based translation detection, IEEE Transactions on Geosciences and Remote Sensing, **40(3)**, 637-650 **(2002)**.